Oncology Research, Vol. 28, pp. 899–911
Printed in the USA.

0965-0407/22 $90.00 + .00
DOI: https://doi.org/10.3727/096504021X16281573507558
E-ISSN 1555-3906
www.cognizantcommunication.com

A Combined Chemical, Computational, and In Vitro Approach Identifies SBL-105 as Novel DHODH Inhibitor in Acute Myeloid Leukemia Cells

Hossam Kamli,* Gaffar S. Zaman,* Ahmad Shaikh,* Abdullah A. Mobarki,† and Prasanna Rajagopalan*‡

*Department of Clinical Laboratory Sciences, College of Applied Medical Sciences, King Khalid University, Abha, Saudi Arabia
†Department of Medical Laboratory Technology, Faculty of Applied Medical Sciences, Jazan University, Jazan, Saudi Arabia
‡Central Research Laboratory, College of Applied Medical Sciences, King Khalid University, Abha, Saudi Arabia

Inhibition of the dihydroorotate dehydrogenase (DHODH) has been successful at the preclinical level in controlling myeloid leukemia. However, poor clinical trials warrant the search for new potent DHODH inhibitors. Herein we present a novel DHODH inhibitor SBL-105 effective against myeloid leukemia. Chemical characteristics were identified by ^{1}H NMR, ^{13}C NMR, and mass spectroscopy. Virtual docking and molecular dynamic simulation analysis were performed using the automated protocol with AutoDock-VINA, GROMACS program. Human-recombinant (rh) DHODH was used for enzyme inhibition study. THP-1, TF-1, HL-60, and SKM-1 cell lines were used. MTT assay was used to assess cell viability. Flow cytometry was employed for cell cycle, apoptosis, and differentiation analysis. Chemical analysis identified the compound to be 3-benzylidene-6,7-benz-chroman-4-one (SBL-105). The compound showed high binding efficacy toward DHODH with a $\Delta G_{binding}$ score of −10.9 kcal/mol. Trajectory analysis indicated conserved interactions of SBL-105–DHODH to be stable throughout the 200-ns simulation. SBL-105 inhibited rh DHODH with an IC_{50} value of 48.48 nM. The GI_{50} values of SBL-105 in controlling THP-1, TF-1, HL-60, and SKM-1 cell proliferations were 60.66, 45.33, 73.98, and 86.01 nM, respectively. A dose-dependent increase in S-phase cell cycle arrest and total apoptosis was observed by SBL-105 treatment in both cell types, which were reversed in the presence of uridine. The compound also increased the differentiation marker CD11b-positive populations in both THP-1 and TF-1 cells, which were decreased under uridine influence. SBL-105, a novel DHODH inhibitor, identified using computational and in vitro analysis, was effective in controlling AML cells and needs attention for further preclinical developments.

Key words: Acute myeloid leukemia (AML); Cell differentiation; DHODH; Drug simulation; In silico

INTRODUCTION

Dihydroorotate dehydrogenase or DHODH, a ubiquitous enzyme is vital for the fourth step of de novo pyrimidine synthesis, where it catalyzes the conversion of dihydroorotate to orotate utilizing ubiquinone as a cofactor. As this reaction is considered exclusive, the enzyme is regarded as essential for the production of uridine monophosphate (UMP)[1]. UMP is the primary building block of pyrimidine biosynthesis, which is again essential for DNA/RNA production. Therefore, inhibition of DHODH leads to a rapid depletion in the UMP stores, finally ending up with the loss in cellular viability[1]. While the cells are proficient in scavenging the extracellular uridine for their survival, the extracellular concentrations are insufficient to sustain life as a replacement to DHODH inhibition[2]. Therefore, targeting DHODH has become an attractive point in clinical conditions, including malignancies[3–5] as well as autoimmune and inflammatory diseases[6].

Acute myeloid leukemia (AML) is often characterized by myeloblast-induced clonal expansion and differentiation[7]. Because of the stem cell-derived hematopoietic origin, AML presents an uncontrolled accumulation of myeloblasts in the bone marrow, blood, and organs, making it more fatal[8]. Currently, the standard therapy uses cytarabine–anthracycline combination with an average success rate of 35%–45% in below 60-year-old patients and 10%–15% for patients above 60 years[9].

Several DHODH inhibitors are under developmental process with clinical trials performed against various diseases, few of which are IMU 838, PP001, and PTC299 against inflammatory bowel disease, autoimmune

Address correspondence to Prasanna Rajagopalan, Ph.D., F.I.C.S., Department of Clinical Laboratory Sciences, Room No. 131, Building C, College of Applied Medical Sciences, Guraiger King Khalid University, Abha, Asir, Saudi Arabia. Tel: +966540924232; E-mail: rajagopalan@kku.edu.sa, prachu.rg@gmail.com

disease, and hematological malignancy, respectively[1]. AG-636, a DHODH inhibitor, is currently under preclinical investigation and dose optimization for AML treatment[1]. DHODH has always been an important target to fight AML. Brequinar, a potent DHODH inhibitor, although it displayed good efficacy in preclinical studies, the results in patients were disappointing[10,11]. A recent study attempted in developing 2-hydroxypyrazolo[1,5-a] pyridine scaffold, which successfully showed it superior to brequinar in terms of efficacy and toxicity[12]. Leflunomide is another interesting DHODH inhibitor drug that was actively tested against several forms of malignancies like leukemia[13], multiple myeloma[14], and melanoma[15]. However, the major drawback with leflunomide was its low potency and lesser half-life. With a focus on DHODH inhibition as a treatment option in myeloid malignancy, few other compounds like BAY2402234 and ASLAN003 have entered the clinical trials. However, a search of novel pyrimidine synthesis inhibitors that could line up for AML treatment is needed. This study, therefore, focused on a combined approach of different disciplines to identify a novel DHODH inhibitor that could be beneficial against myeloid malignancies.

MATERIALS AND METHODS

Materials

Reagents and chemicals were purchased from Sigma-Aldrich (St. Louis, MO, USA). THP-1, TF-1, HL-60, and SKM-1 cell lines were from ATCC (American Type Culture Collection, Rockville, MD, USA). Annexin V and cell cycle assay reagent were from Merck Millipore (Burlington, MA, USA). DHODH enzyme assay kit was from R&D Systems (Minneapolis, MN, USA). Phycoerythrin (PE)-conjugated anti-CD11b antibody was from eBioscience™, ThermoFisher Scientific (Waltham, MA, USA).

Synthesis of SBL-105

The reaction mixture containing tolualdehyde (0.02 mole, 2.35 ml), methyl acrylate (0.30 mole, 3.3 ml), DABCO (0.003 mole, 0.336 g), and silica gel (>200 mesh; 2.5–5 g) was monitored by thin layer chromatography. After the completion of the reaction, the reaction mixture was diluted with ethyl acetate (4 × 10 ml) and filtered. The filtrate was washed successively with 2N HCl solution, aqueous saturated sodium bicarbonate solution, and water. The organic layer was dried over anhydrous sodium sulfate and then purified by column chromatography (silica gel; 5% ethyl acetate in hexane) to obtain a compound of alkyl-α-methylene-β-(4-methyl-aryl) propanoate. The α-methylene-β-phenyl-propanoate was stirred with hydrobromic acid and catalytic amount of concentrated sulfuric acid. The reaction was extracted with ether and washed with saturated sodium bicarbonate solution and water. The organic layer was dried over sodium sulfate. The solvent was evaporated, and the residue was purified by column chromatography using silica gel, 5% ethyl acetate in hexane to obtain a compound of methyl-(2,*Z*)-2-bromo methyl 3-aryl-prop-2-enoate. The bromo methyl propenoate (0.006 mole, 1.014 g) was treated with (0.006 mole, 0.864 ml) napthanol in the presence of potassium carbonate in acetone at reflux temperature for 3 h. The reaction mixture was diluted with ether, washed with water, dried, and ether layer evaporated. The residue was purified by column chromatography using silica gel, 3% ethyl acetate in hexane to obtain a compound of 3-(4-methyl)-aryl-2-naphthoxy methyl prop-2-enoate. The naphthoxy ester was hydrolyzed by using potassium hydroxide in aqueous 1,4-dioxan at room temperature. The reaction mixture was acidified, and the precipitate was purified by recrystallized to give 3-(4-methyl) aryl-2-naphthoxy methyl prop-2-enoic acid. The phenyloxy propenoic acid (0.001 mole, 0.33 g) was treated with (0.001 mole, 0.21 ml) TFAA, and the reaction mixture was refluxed in dichrolomethane for 1 h. The reaction mixture was diluted with ether, and washed with aqueous saturated sodium bicarbonate solution and water. The ether layer was dried over anhydrous sodium sulfate, and the solvent was evaporated. The crude compound was purified by column chromatography by using silica gel, 3% ethyl acetate in hexane to give 3-(4-methyl) benzlidene-6,7-benz-chroman-4-one. The compound was internally referred as SBL-105.

In Silico Protein–Ligand Docking Analysis

The three-dimensional structure of DHODH was retrieved from PDB databank (PDBid: 6qu7). The structure was prepared before docking studies using a receptor preparation script from AutoDock tools. Structures of known DHODH inhibitors were retrieved from the PubChem database in SDF format. SBL-105 structure in SDF format was converted to SYBYL-TRIPOS (mol2) format using BIOVIA-Discovery Studio Visualizer. Converted mol2 files were then converted to AutoDock-VINA format using ligand preparation script from AutoDock tools. Docking was performed using the automated protocol developed by SiBIOLEAD. Briefly, a docking box was generated based on the information gained from the DHODH structure complexed with BAY 2402234 (6qu7) by selecting two amino acid residues on either side of the active site. AutoDock-VINA program was used with standard docking mode (i.e., exhaustiveness = 8). Protein–ligand interactions were analyzed using PLIP protein–ligand analysis package.

Simulation Analysis

Atomistic molecular dynamics (MD) simulation was performed using the GROMACS simulation package.

The simulation was carried out in WebGro MD simulation tool (https://simlab.uams.edu/) that automates job submission and result analysis in process. In brief, docked protein–ligand complex was prepared for GROMACS MD simulation, and ligand topology was generated using the PRODRG module (http://prodrg1.dyndns.org/submit.html), which was supplied as an input for WebGro job submission. A triclinic simulation box was constructed and filled with SPC water molecules, and NaCl was added as counterions. In order to mimic physiological conditions, 0.15 M salt (NaCl) was added to the simulation box. Before the actual MD run, a simulation system containing protein–ligand complex, water molecules, and ions was minimized for 5,000 steps using the Steepest Descent method and equilibrated under NVT/NPT protocol. MD run was performed for 200 ns, and trajectories were analyzed as a part of WebGro tool. Simulation figures were plotted using VMD and BIOVIA Discovery Studio.

DHODH Enzyme Assay

The assay was carried out using an absorbance-based kit as per the manufacturer's instructions. Briefly, 0.02 µg of human-recombinant (rh) DHODH at final concentration in the assay buffer containing 50 mM Tris, 150 mM KCl, 0.1% Triton® X-100, pH 8.0 was added in a 96-well clear-bottom plate. After adding the desired concentrations of SBL-105, the reaction was initiated by addition of the substrate mixture that contained 2 mM L-dihydroorotic acid, 0.2 mM decylubiquinone, and 0.12 mM DPIP in assay buffer. Absorbance was measured at 600 nM. Percentage inhibition was calculated, and IC_{50} value was determined using GraphPad Prism 6.0 software.

Cell Culture

RPMI-1640 medium was used for the growth of THP-1 and TF-1 cells. Cells were grown as per standard protocols in growth media supplemented with 10% fetal bovine serum (FBS), 100 U/ml of penicillin, and 100 U/ml streptomycin. Assays were carried out when cells reached around 80% confluency state.

Cell Proliferation Assay

Cell proliferations were assessed using MTT assay as described elsewhere[16]. AML cells (5×10^3 cells/well) were grown in a 96-well tissue culture plate in regular growth medium. Cells were treated with respective concentrations of SBL-105 for 72 h. After removing the medium, 100 µl of MTT (1 mg/ml) was added as a replacement for medium and further incubated for 4 h. Formazan products were dissolved in 200 µl of dimethyl sulfoxide (DMSO), and absorbance at 560 nm was measured. Percent inhibition was calculated using GraphPad Prism 6.0 for the GI_{50} values.

Cell Cycle Analysis

The assay was carried out with a cell cycle assay kit according to the manufacturer's instructions as follows. AML cells, at a density of 5×10^5 cells per well, were seeded in a six-well plate and incubated for 24 h. After addition of respective concentrations of SBL-100 with or without uridine, the incubation was carried out for another 72 h. After a couple of washes with sterile phosphate-buffered saline (PBS), 50 µl of cell cycle assay reagent was added, and then incubated in the dark for 15 min and washed with wash buffer for two times and resuspended in HBSS buffer. Ten thousand events were acquired on a Guava easyCyte™ flow cytometer, and the data were analyzed with ExpressPro Software from Millipore. The percentage of cell populations in the S phase of the cell cycle was presented.

Detection of Apoptosis

Annexin V detection kit was used for this assay as per the manufacturer's instructions. THP-1 or TF-1 cells (5×10^5) were grown in six-well plates and treated with respective concentrations of SBL-105, with or without uridine, followed by 5% CO_2 incubation at 37°C for 48 h. Postincubation period, cells were harvested, washed with kit buffer, and incubated with 0.25 µg/ml annexin V reagent for 15 min in the dark. After a couple of washes, cells were resuspended in kit buffer containing 0.5 µg/ml propidium iodide. Ten thousand events were acquired on a Guava easyCyte™ flow cytometer. Data analysis was carried out with InCyte software to differentiate healthy and apoptotic cells (early and late apoptosis) and presented using Graphpad Prism software, version 6.0 (La Jolla, CA, USA).

Cell Differentiation Analysis

THP-1 or TF-1 cells were plated in six-well plate with complete media and treated with 100 nM SBL-105 in the presence or absence of uridine. Following a 96-h incubation period, cells were washed twice with PBS, and added with 0.5 µg/ml fluorescein isothiocyanate (FITC) conjugated, anti-CD11b antibody, and incubated for 20 min in dark. After a couple of washes in PBS, cells were resuspended in HBSS buffer, and 10,000 events were acquired in Guava easyCyte™ flow cytometer. The data were analysed using InCyte Software from Millipore. The percentage of positive CD11b cell population was presented.

Statistical Analysis

Statistical analyses were performed using GraphPad Prism 6.0. Results were expressed as the mean ± SD. Data were analyzed using analysis of variance (ANOVA) followed by multiple comparisons. Values of $p \leq 0.05$ were considered significant.

RESULTS

Chemical Characteristics of SBL-105

The proton nuclear magnetic resonance (^{1}H NMR) spectrum is shown in Figure 1a. Analysis revealed a doublet at 9.44 δ for a single proton indicates the vinylic proton (Table 1a). A doublet at 7.93 δ for one proton, a singlet at 7.91 δ for one proton, a doublet at 7.77 δ for one proton, a doublet of a triplet at 7.66 δ for one proton, and another doublet of triplet at 7.45 δ for one proton, a quartet at 7.25 δ for four protons, a doublet at 7.09 δ for one proton indicate the 10 aromatic protons (Table 1a). A doublet at 5.4 δ for two protons indicates the naphthoxy-methylene protons, and a singlet for three protons at 2.4 δ indicates the Ar-CH3 group (Table 1a). Figure 1b is the carbon nuclear magnetic resonance spectroscopy (^{13}C NMR) of the compound. The procedure shows sharp infrared (IR) absorption at 1665, 1596 cm^{-1}, and the disappearance of broad band around 3430 cm^{-1} indicates that this is an aromatic unsaturated ketone. Table 1b shows δ values (ppm). From the mass spectroscopy (Fig. 1c) inference, the m/e value of the compound corresponds to the molecular weight of 300.3, and elemental analysis agrees with the molecular formula of compound, Calcd: C, 84.07%; H, 5.37%; Found: C, 84.15%; H, 5.38% (Table 1c). From these data, the compound was identified to be 3-benzylidene-6,7-benz-chroman-4-one (Fig. 1c), and internal reference for the compound was given as SBL-105.

In Silico Docking Showed SBL-105 to Profoundly Bind DHODH

We evaluated the docking efficacy of SBL-105 with DHODH enzyme using an in silico computational approach. First, the enzyme's energy binding pocket was determined in the crystal structure using known DHODH inhibitor BAY-384405123 (data not presented). Our docking analysis predicted SBL-105 to exactly bind to the same energy pocket (Fig. 2a and b). The compound had an excellent binding affinity toward the crystal structure of DHODH enzyme with a binding energy of −10.90 Kcal/mol (Fig. 2c). PLIP analysis for critical interacting residues included PRO52, ALA55, HIS56, VAL134, ARG136, VAL143, THR285, SER305, and TYR356 (Fig. 2d).

MD Simulation Predicts Stable Binding of SBL-105 With DHODH

To predict the stability of SBL-105 binding to DHODH, we conducted 200-ns fully solvated atomistic MD simulation using WebGro simulation tool (https://simlab.uams.edu/). Results indicate a stable binding of protein–ligand complex; root mean square deviation (RMSD) of ligand

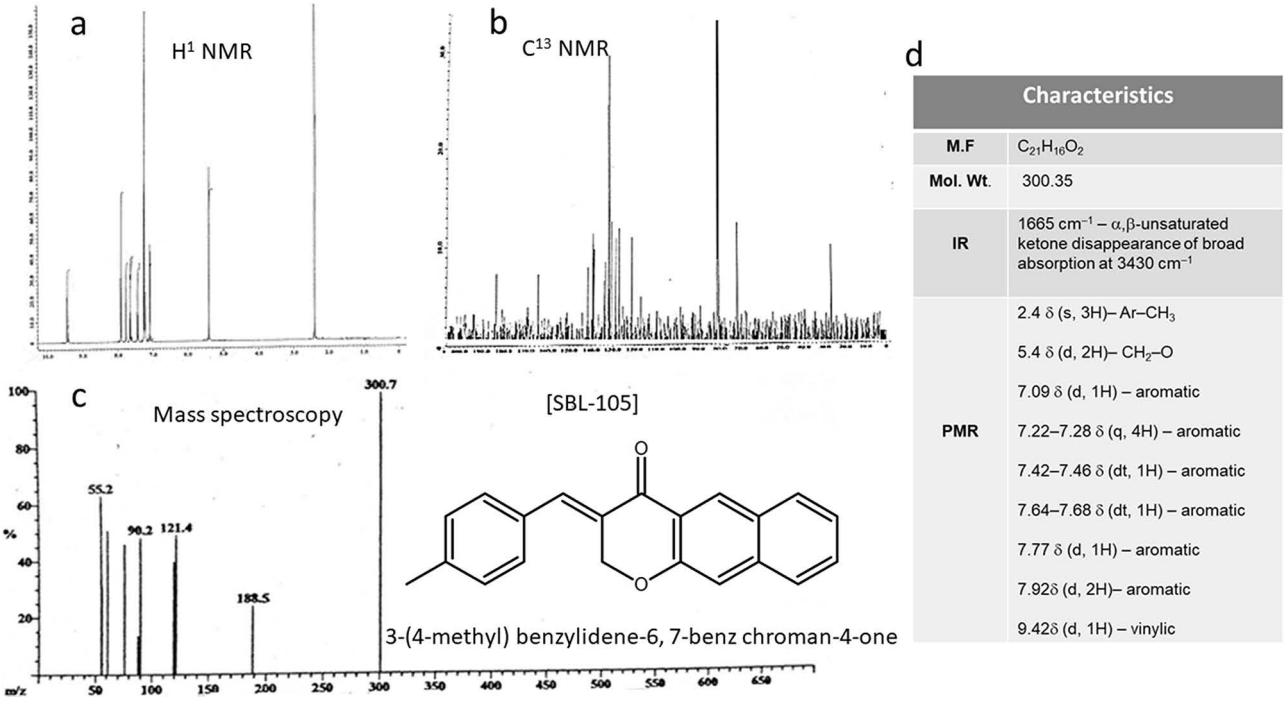

Characteristics	
M.F	$C_{21}H_{16}O_2$
Mol. Wt.	300.35
IR	1665 cm^{-1} – α,β-unsaturated ketone disappearance of broad absorption at 3430 cm^{-1}
PMR	2.4 δ (s, 3H)– Ar–CH_3
	5.4 δ (d, 2H)– CH_2–O
	7.09 δ (d, 1H) – aromatic
	7.22–7.28 δ (q, 4H) – aromatic
	7.42–7.46 δ (dt, 1H) – aromatic
	7.64–7.68 δ (dt, 1H) – aromatic
	7.77 δ (d, 1H) – aromatic
	7.92δ (d, 2H)– aromatic
	9.42δ (d, 1H) – vinylic

Figure 1. Chemical elucidation for the synthesized benzylidene chromanone compound SBL-105. (a) Proton nuclear magnetic resonance (NMR) of the synthesized compound. (b) Carbon nuclear magnetic resonance spectroscopy of SBL-105. (c) Mass spectrum confirming the structure, molecular weight, and IUPAC (International Union of Pure and Applied Chemistry) name of the synthesized compound SBL-105. (d) δ values based on NMR results and elemental analysis depicting chemical properties of the compound.

Table 1a. Mass Spectrum Analysis of SBL-105 Confirming the Physical and Chemical Characteristics

Compound	Aromatic Region (δ)	H_a (δ)	H_b (δ)	OCH_3 (δ)	CH_3 (δ)
SBL-105	7.93 (d, 1H, J = 7.6 Hz), 7.91 (d, 1H, J = 7.5 Hz), 7.77 (d, 1H, J = 7.5 Hz), 7.68–7.64 (dt, 1H, J = 7.8 Hz), 7.46–7.40 (dt, 1H, J = 7.8 Hz), 7.28–7.22 (q, 4H, J = 7.8 Hz), 7.09 (d, 1H, J = 7.6 Hz)	9.44 (d, 1H, J = 10 Hz)	5.40 (d, 2H, J = 1.6 Hz)	–	2.40 (s, 3H)

Table 1b. ^{1}H NMR Values of the Synthesized Compound SBL-105

Compound	δ Values (ppm)
SBL-105	21.56, 67.68, 76.86, 77.11, 77.37, 118.83, 125.08, 126.57, 128.56, 129.54, 130.08, 131.48, 131.97, 136.98, 137.41, 139.76, 163.19, 182.73

Table 1c. ^{13}C NMR Values of the Synthesized Chromanone SBL-105

Compound	Yield (%)	Melting Point (°C)	IR (cm^{-1})	MS (70 ev) M/Z (M^+)	Molecular Formula	Elemental Analysis Calcd/Found C	H
SBL-105	94	140	1665 1596	300.7	$C_{21}H_{16}O_2$	84.07% 84.50%	5.37% 5.38%

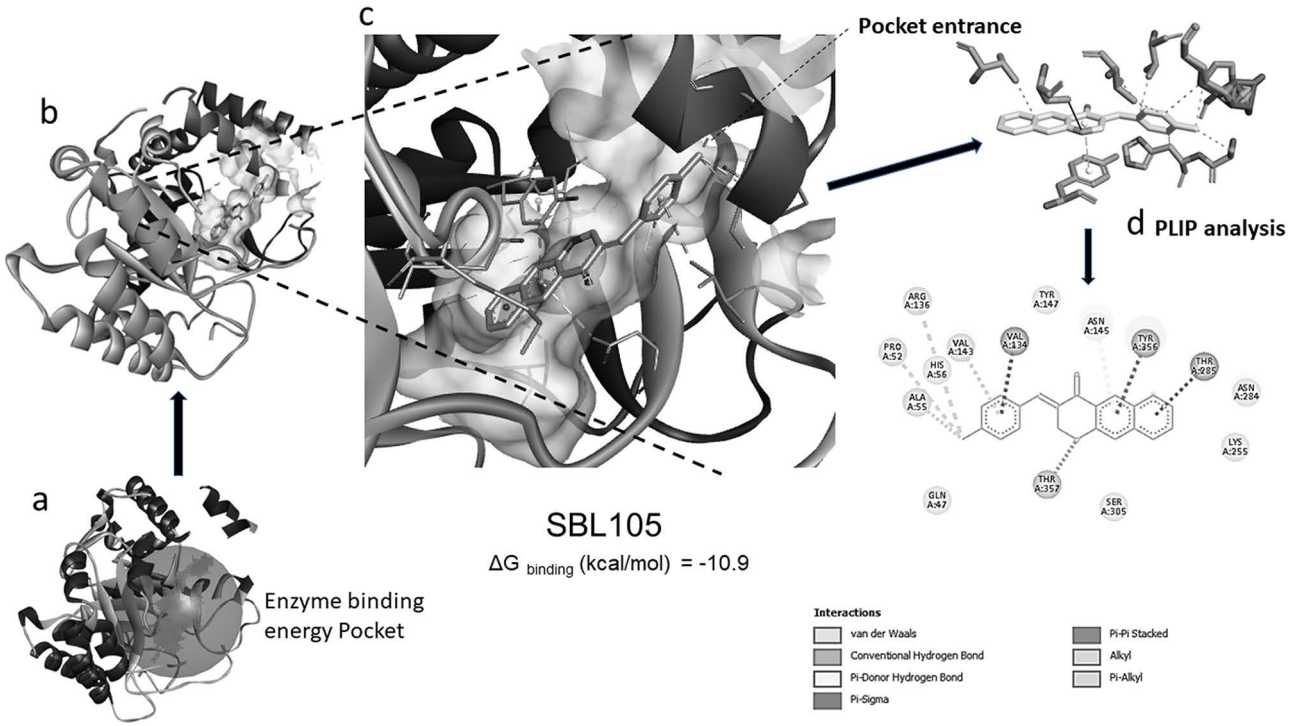

Figure 2. Binding efficacy of SBL-105 to dihydroorotate dehydrogenase (DHODH) enzyme. (a) Enzyme's energy binding pocket. (b) In silico docking shows inhibitory efficiency of SBL-105 in crystal structure DHODH enzyme. (c) Magnified image of the active site shows SBL-105 binding position with associated ligand–protein interactions. (d) A two-dimensional analysis of the protein–ligand amino acid interactions involved in SBL-105 binding with DHODH.

(SBL-105) superimposed with initial conformation indicates a stable binding throughout the simulation (Fig. 3a). RMSD of the ligand shows a sharp rise in the beginning of the simulation and settles immediately after 10 ns, indicating a favorable binding environment for SBL-105 at DHODH (Fig. 3a). Trajectory analysis at different time points indicates conserved interactions of SBL-105 with residues of DHODH (Fig. 3b). Furthermore, the average number of hydrogen bonds between ligand (SBL-105) and DHODH stays stable throughout the 200-ns simulation, suggesting a stable binding of SBL-105 within the DHODH pocket (Fig. 3c). Similarly, trajectory analysis video of 200-ns simulation clearly shows a stable binding of SBL-105 with DHODH (data not presented, available on request).

SBL-105 Inhibits DHODH Enzyme In Vitro and Exerts Antiproliferative Effects

SBL-105 effectively inhibited the full-length DHODH enzyme with an IC_{50} value of 48.48 nM (Fig. 4a). To investigate the efficacy of SBL-105 on myeloid leukemia cell proliferations, the AML THP-1 and erythroleukemia myeloid progenitor TF-1 cells were used. SBL-105 controlled the proliferations of THP-1 cell with a GI_{50} value of 60.66 nM, and TF-1 cells with GI_{50} value of 45.33 nM (Fig. 4b). GI_{50} values for HL-60 and SKM-1 cells were 73.98 and 86.01 nM, respectively (Fig. 4b). Since exogenous uridine concentrations offer an alternative pathway (salvage pathway) for DNA synthesis, the need for DHODH is negated under uridine influence. Therefore, the cell viabilities of SBL-105-treated THP-1 and TF-1 cells were analyzed in the presence of 100 μM uridine. Based on the GI_{50} values, we selected one low and mid concentration, which was 10 and 100 nM SBL-105 to be tested under uridine influence. While untreated DMSO control cells had 96% cell viability, the 10 nM SBL-105-treated THP-1 had 77.3% viable cells and the 100 nM-treated THP-1 had 34.66% viable cells (Fig. 4c). Uridine presence increased the viability of these cells to 94.64% and 96.05%, respectively, for 10 and 100 nM SBL-105 treatments (Fig. 4c). Similarly, the untreated control TF-1 cells had 96.07% viable cells (Fig. 4d). Treatment with 10 and 100 nM SBL-105 decreased the TF-1 cell viability to 78.66% and 49.8%, respectively. In the presence of 100 μM uridine, the 10 nM-treated TF-1 cells had 95.56% viability and 100 nM SBL-105-treated cells had 98.38% viability (Fig. 4d).

Alteration of the Cell Cycle and Induction of Apoptosis by SBL-105 in Myeloid Leukemia Cells

Treatment with 100 nM SBL-105 increased the S phase cell population from 15.06% to 52.19% with

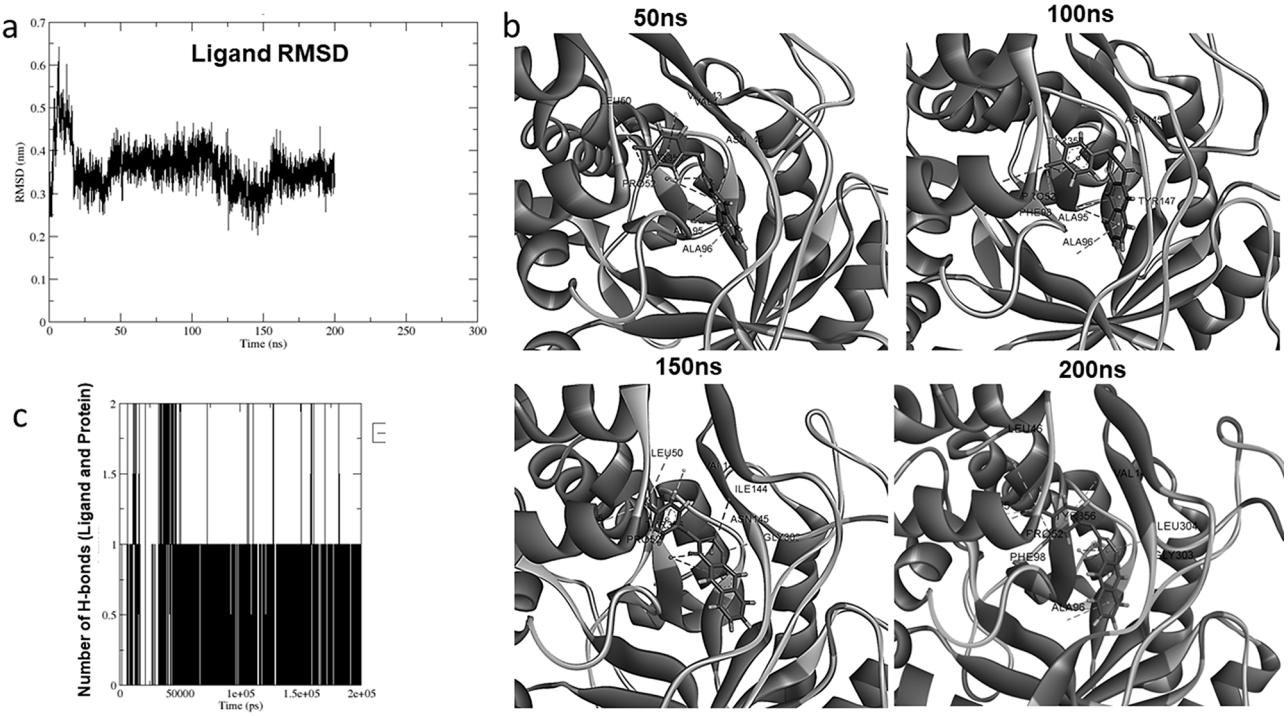

Figure 3. Stability testing by molecular dynamic simulation analysis. (a) Root mean square deviation (RMSD) of SBL-105 when superimposed with initial conformation. (b) RMSD of SBL-105 at different time points with interacting residues. (c) Interaction of average hydrogen bonds with SBL-105 throughout 200-ns simulation indicating the ligand stability in the molecular dynamics (MD) analysis.

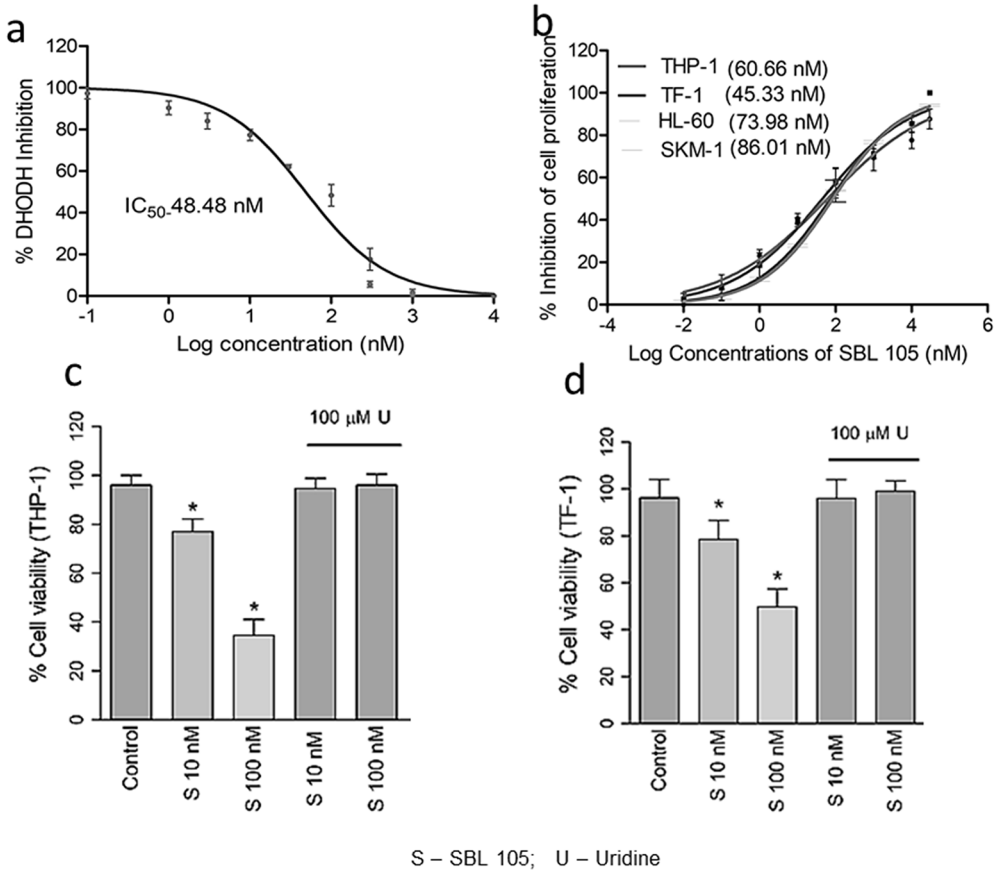

Figure 4. In vitro profile of SBL-105. (a) IC_{50} of SBL-105 against full-length human DHODH enzyme. (b) GI_{50} of SBL-105 in controlling proliferation of THP-1, TF-1, HL-60, and SKM-1 cells. (c, d) Cell viability assay of (c) THP-1 and (d) TF-1 cells when treated with 10 and 100 nM SBL-105 in the presence or absence of 100 μM uridine (U). The lost viability of these cells when treated with SBL-105 was restored in the presence of uridine. Data presented as mean ± SD from three independent experiments. *$p \leq 0.05$ when compared to untreated control.

respect to untreated control in THP-1 cells (Fig. 5a). The 10 nM compound-treated cells had 35.56% cells in the S phase (Fig. 5a). Treatment with 10 nM SBL-105 to TF-1 cells increased the S phase population from 16.53% to 41.33%, while 100 nM treatment further increased it to 51.16% (Fig. 5b). However, in presence of 100 μM uridine, both treatments in either type of the cells have the S phase populations close to their respective controls (Fig. 5a and b). When checked for the apoptosis-inducing property of SBL-105, 100 and 10 nM SBL-105 treatment increased early and late phase apoptosis in both THP-1 and TF-1 cells (Fig. 6a and b). The 100 nM SBL-105 treatment increased the total apoptosis in THP-1 cells to 27.12% from 2.52% of the control cells (Fig. 6a). The 10 nM treatment showed 18.82% total apoptosis in these cells (Fig. 6a). The 10 nM treatment increased the total apoptotic cell population to 20.86% from 3.91% as that of control in TF-1 cells (Fig. 6b). Increase in the treatment dose to 100 nM further elevated total apoptosis in these cells to 32.30% (Fig. 6b). In the presence of uridine, the total apoptosis of SBL-105-treated THP-1 and TF-1 cells was observed close to their respective controls, irrespective of the treatment concentrations (Fig. 6a and b).

SBL-105 Promotes Cell Differentiation in Myeloid Leukemia Cells

To understand if there was any effect of the compound on the cell differentiation, THP-1 and TF-1 cells were treated with 100 nM SBL-105 in the presence or absence of 100 μM uridine and analyzed for expression of CD11 b, the differentiation marker. As observed in Figure 7, 100 nM SBL-105 treatment of THP-1 cells increased the CD11b percentage to 39.21% from 8.35% as that of untreated control. For TF-1 cells, it was 47.79% CD11b-positive cells when treated with 100 nM SBL-100, while the respective control had 7.13% (Fig. 7). In both cell types, under uridine influence, a substantial decrease in the CD11b percentage was observed, with 15.63% and 18.81% for THP-1 and TF-1 cells, respectively (Fig. 7).

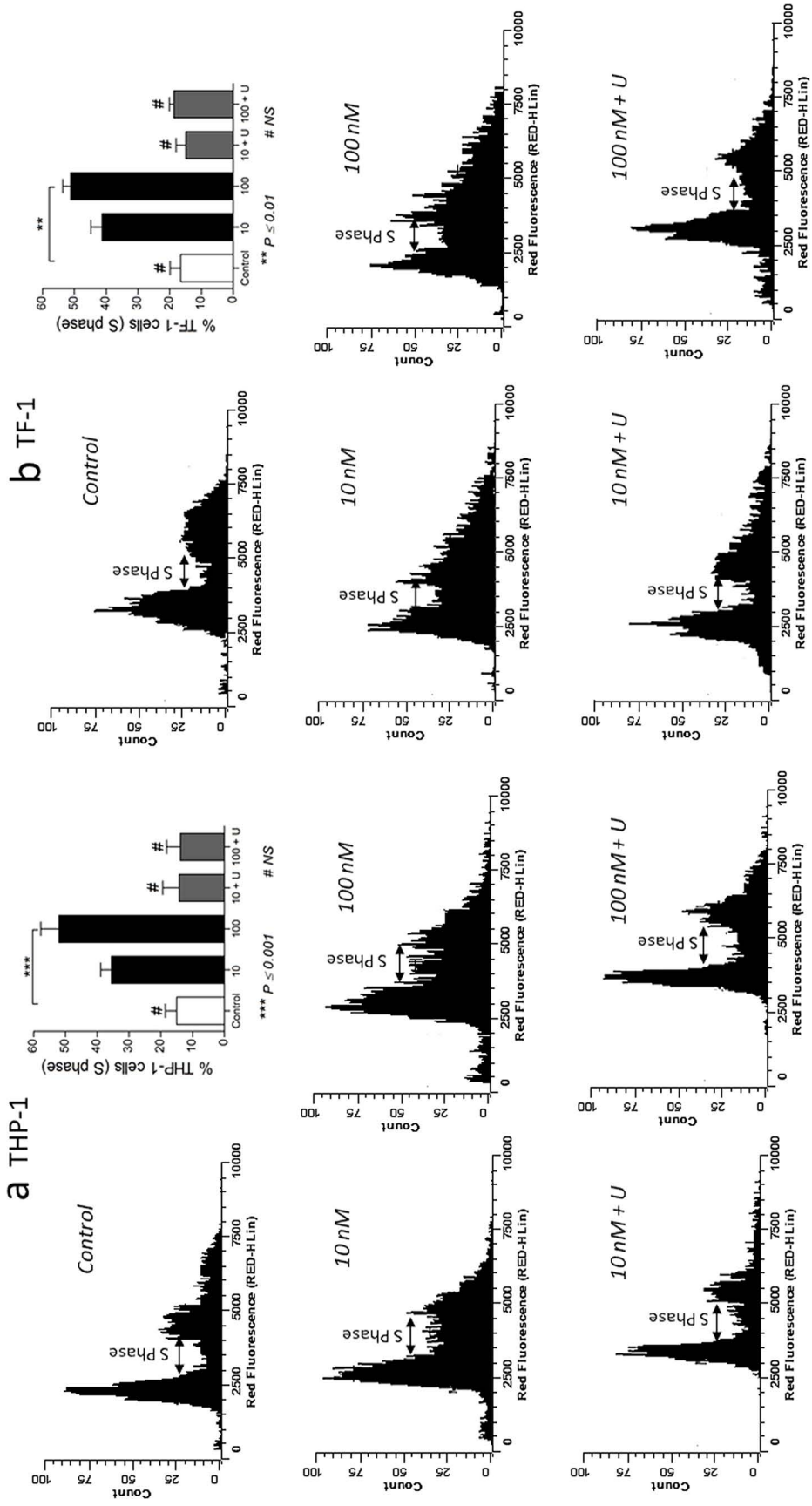

Figure 5. Cell cycle analysis of acute myeloid leukemia (AML) cells with SBL-105 treatments. Increase in the S phase percentage of cell cycle observed in (a) THP-1 and (b) TF-1 cells when treated with different doses of SBL-105. Addition of 100 μM uridine (U) reduced S phase cell populations in these cells. Histograms represent mean ± SD percentage of S phase cells from three independent experiments mean.

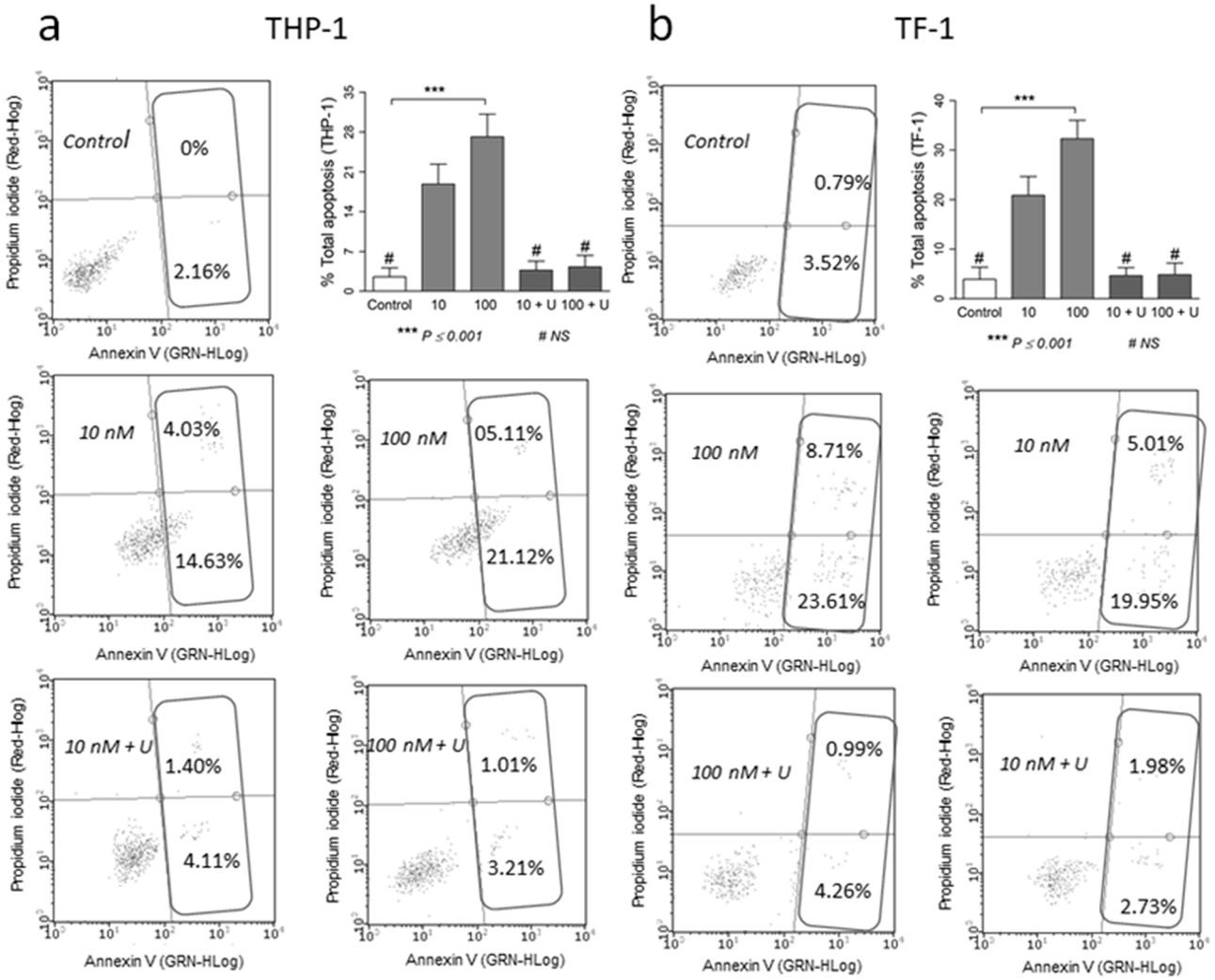

Figure 6. Enumeration of apoptosis by SBL-105 treatment. Annexin V assay shows apoptotic cell populations in (a) THP-1 and (b) TF-1 cells with different doses of SBL-105 treatments. Representative histograms from three different experiments are presented. The numerical values in the lower right quadrant indicate early apoptotic cells, and values in upper right quadrant represent late apoptotic cells. Total apoptotic cells presented as histograms are mean ± SD.

Effect of SBL-105 in Physiological Uridine Concentrations

We next checked the activity of SBL-105 in TF-1 and THP-1 cell proliferation under physiological uridine concentration of 5 μM. The antiproliferative effects were reduced in the presence of physiological uridine concentrations in both AML cell types (Fig. 8a and b). When treated with salvage pathway pyrimidine blocker, dipyridamole, we observed the antiproliferative activities of SBL-105 were almost restored (Fig. 8a and b).

DISCUSSION

Attempt with DHODH inhibition to manage diseases has been reported in previous literature[17]. Brequinar sodium, leflunomide, or teriflunomide was tested for anticancer efficacies mediated by DHODH inhibition[18,19]. Teriflunomide was also approved for treatment against multiple sclerosis and rheumatoid arthritis. However, the efficacy of this compound had a weak DHODH inhibition with IC_{50} values in the micromolar range[19]. Therefore, search for a new potent class of DHODH inhibitors is in demand.

The 3-benzylidene chroman-4-ones are a class of small molecules with unique oxygen heterocycles. These molecules are reported to be an integral part of many natural products and biologically active molecules[20]. A very close similarity of benzylidene chromanones could be related to the naturally occurring compounds such as flavanones, flavones, chromones, and coumarins. The established biological activity of these naturally occurring compounds

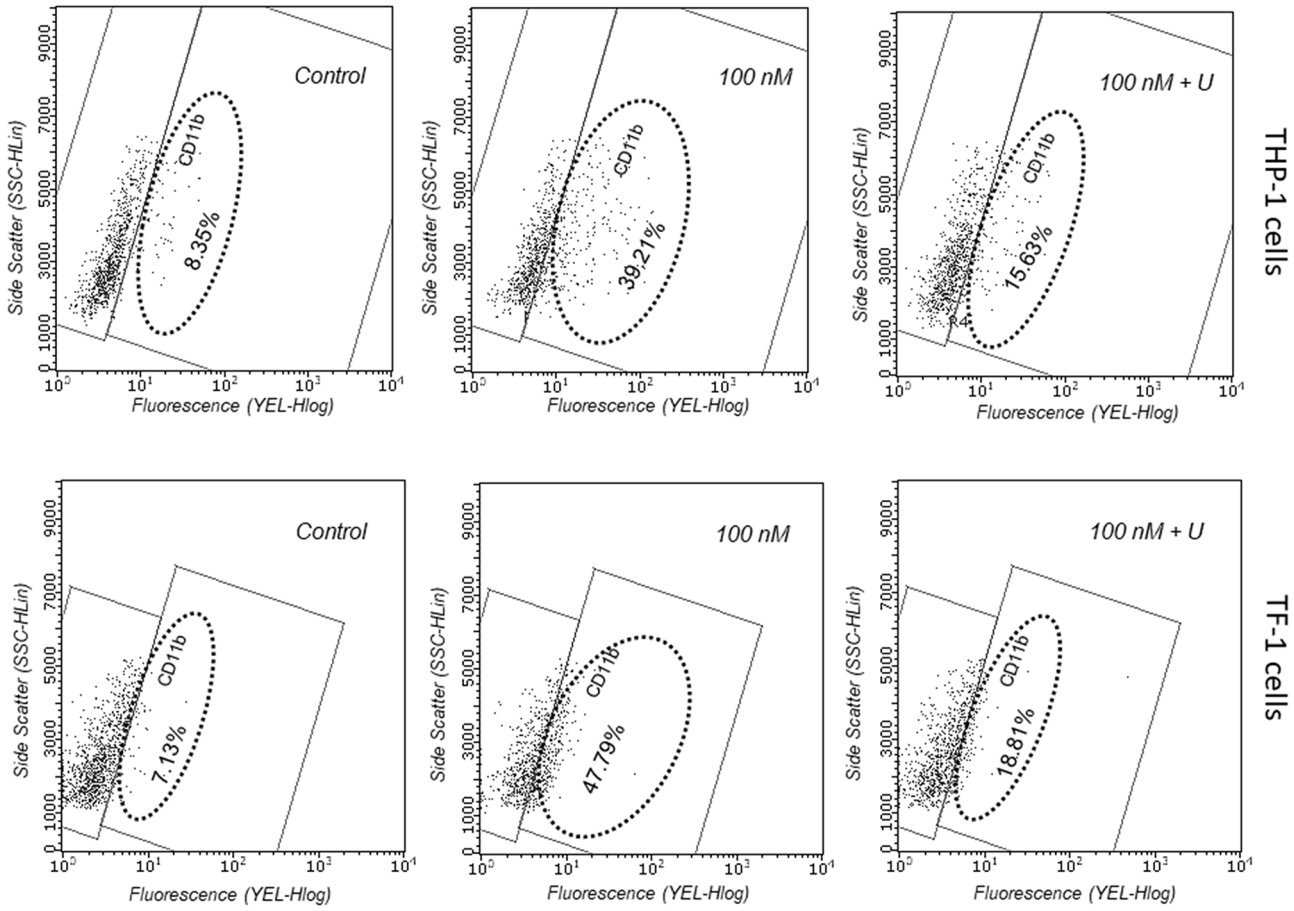

Figure 7. Flow cytometry analysis for the differentiation marker CD11a in THP-1 and TF-1 cells when treated with 100 nM SBL-105 in the presence or absence of 100 μM uridine (U). The numerical values indicate mean ± SD percentage CD11b-positive cells from three experiments.

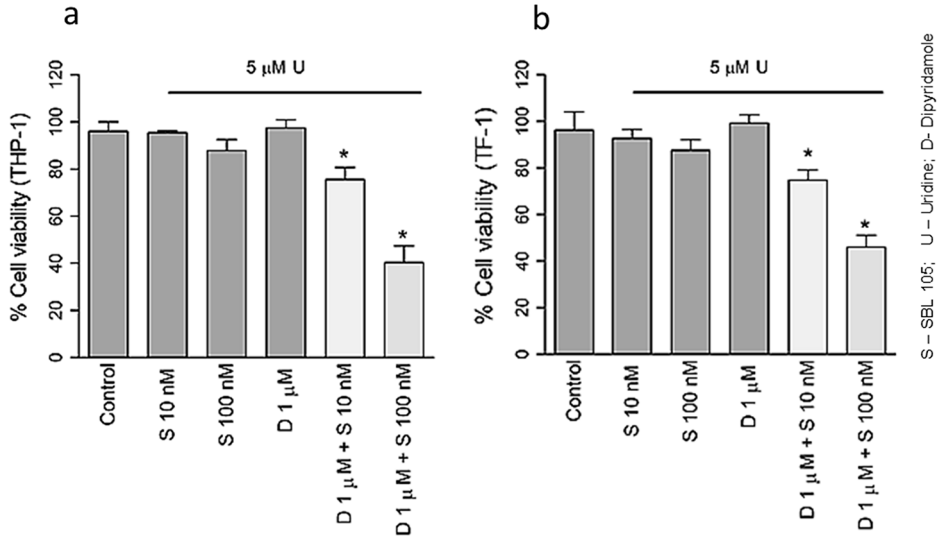

Figure 8. (a, b) Cell viability assay of (a) THP-1 and (b) TF-1 cells when treated with 10 and 100 nM SBL-105 in the presence or absence of 5 μM uridine (U). Both concentrations of SBL-105 did not have an effect on the cell viability of AML cells. Addition of 1 μM dipyridamole to 10 and 100 nM SBL-105 decreased the AML cell viabilities in a dose-dependent way, while dipyridamole alone had no effect on the AML cell viability. Data are presented as mean ± SD from three independent experiments. *$p \leq 0.05$ when compared to untreated control.

possessing a chroman ring system[21] suggested the synthesis of 4-chromanones[22]. The common occurrence of basic side chains in therapeutically active compounds deemed it worthwhile to incorporate the basic group into chromanones to evaluate biological activities. We therefore synthesized such derivatives to be evaluated for their biological efficacy. Our initial in silico screening (data not shared) identified 3-benzylidene-6,7-benz-chroman-4-one (SBL-105) to have excellent binding efficacy to the DHODH enzyme, which was further evaluated against AML in this study (Fig. 9).

Toward identifying the binding mode and stability, in this study we modeled the interactions of SBL-105 with DHODH. Experimental structure of DHODH bound with a known inhibitor BAY-384405123 identified the active and druggable regions of DHODH. The region between the two helices (between residues Leu42 and Ala52) formed a small pocket where BAY-384405123 was shown to bind. Therefore, our modeling studies also focused on the same region. SBL-105 was predicted to bind to the same active region in DHODH, with a relatively higher affinity compared with the BAY compound. Although docking energies show a good fit, stability of the ligand–protein complex is crucial in determining the activity of the molecule. With that regard, MD simulation analysis of SBL-105 bound with DHODH was performed. SBL-105 showed a stable binding, interacting with crucial amino acids throughout the 200-ns simulation, suggesting ligand stability and eventually its inhibitory activity against the DHODH.

Our in vitro findings demonstrated IC_{50} value in the nanomolar range for DHODH enzyme inhibition. These results were almost merely translated in the antiproliferation assay when tested in two types of AML cell lines. Reversal of the activity in the presence of uridine also confirmed the involvement of the DHODH pathway for antiproliferation effects by SBL-105, which were in accordance with reported literature[23]. With the well-known fact that cell proliferation is tightly regulated through cell cycle, we evaluated SBL-105 on cell cycle changes in THP-1 and TF-1 cells. Our results were in agreement with other researchers that DHODH inhibition results in S phase arrest

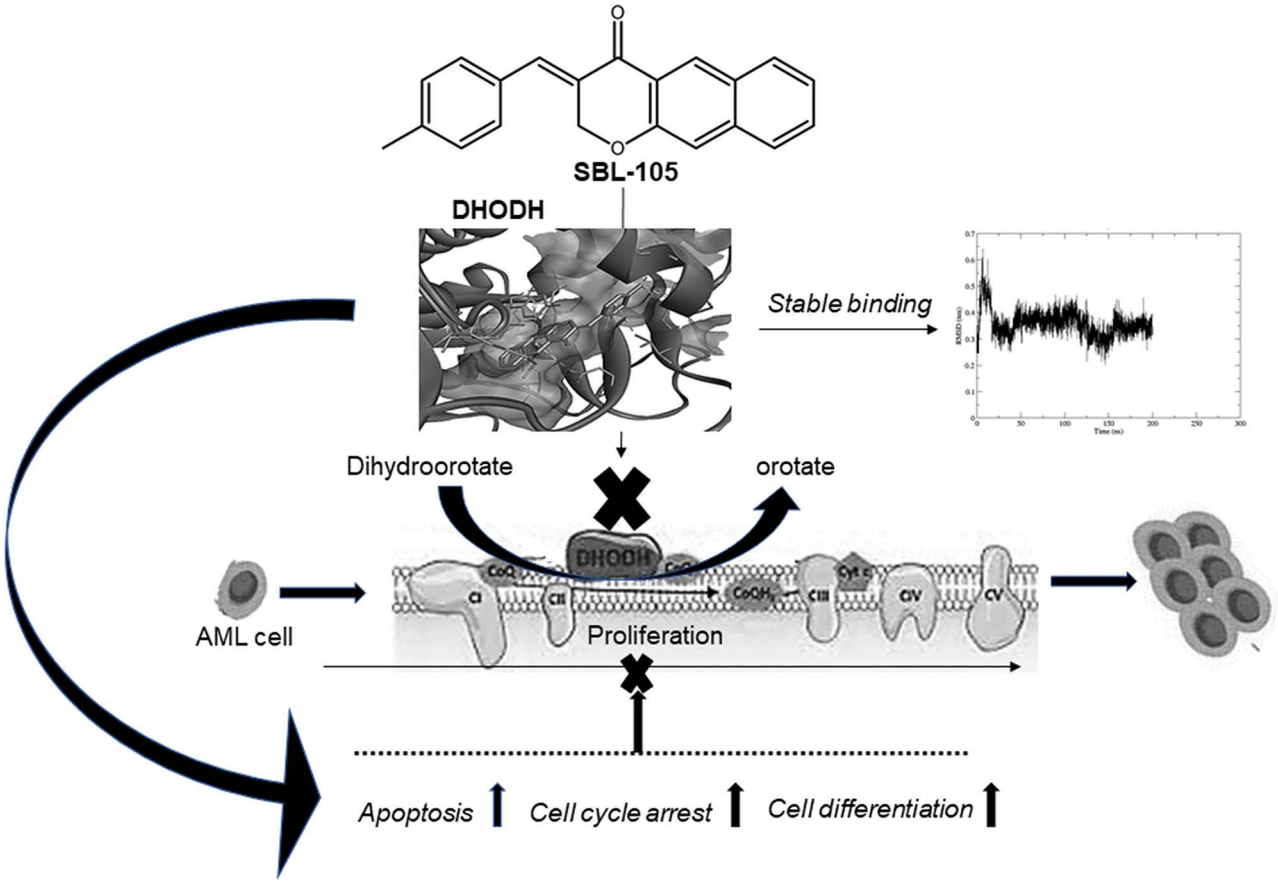

Figure 9. In silico docking analysis predicted SBL-105 to profoundly bind DHODH enzyme. The ligand–protein complex stability was confirmed with MD simulation analysis. SBL-105 favored the apoptosis and cell cycle arrest and promoted cell differentiation to reduce proliferation of AML cells.

of the cell cycle, which would be revered by exogenous uridine[24]. Cell cycle also serves as an important regulator or checkpoint to decide the fate on cell survival. Studies have shown cell cycle arrests preceeds cell death via apoptosis[25]. Our results agreed to the above postulations where distinct apoptosis and cell cycle arrest were observed with SBL-105 treatments in both AML cell types.

Differentiation therapy has been attempted for phenotypic alterations of malignant cells[26]. The essential role of DHODH in AML survival and differentiation is also reported[27]. Studies have analyzed RNA sequencing data from 173 patients to prove that DHODH is one of the key regulators of cell proliferation and differentiation in AML[28]. On the other hand, several reports suggest CD11b as an important marker for cell differentaition in AML cells, which was evaluated as a prognostic marker of disease progression[29,30]. Our observations of elevated CD11b marker with SBL-105 treatments suggested the improvement of AML differentation was effected by the compound, while constitutively inhibiting the proliferation via cell cycle arrest and subsequent apoptosis.

Although preclinically DHODH inhibitors have performed promising in vitro and in vivo activity on solid tumors, some of them have reduced efficacy in clinical trials, probably because cancer cells exploited the pyrimidine salvage pathway to survive[31]. Research shows that efficacy of brequinar sodium (DUP-785; brequinar) was affected in presence of the physiological uridine concentration of 5 μM, which could be partially reversed in the presence of the nucleoside transport inhibitor, dipyridamole[32]. The same study also showed some additive effects when brequinar was combined with 5-fluoro uracil, which could not be effective in the presence of physiological uridine concentration[32]. However, there are other studies that show that blocking the salvage pathway of pyrimidine synthesis and/or by combination of known anticancer agents could bring out an additive or synergistic effect in increasing apoptosis of AML cells with DHODH inhibitor treatments at physiological uridine concentrations[31]. In this research, although our preliminary area of focus was to show a new class of small molecules effective against AML by DHODH inhibition, it is vital to consider the efficacy of our compound in the physiological uridine concentration. Our results were in favor of the later report that a combined treatment with dipyridamole would maintain the efficacy of SBL-105 even in presence of physiological uridine concentrations, while dipyridamole alone was not effective. The limitation of this study is that it focused on the preliminary identification of a new class of DHODH inhibitors through computational and in vitro analysis. However, the performance of SBL-105 in in vivo preclinical conditions and clinical trials has to be tested for successful completion of SBL-105 as a therapeutic candidate against AML. Identifying a class of analogs of SBL-105 and testing them individually and in combination with known chemotherapeutics against AML in preclinical and clinical conditions could be the future direction of our preliminary investigation.

CONCLUSION

In summary, our findings identify SBL-105 as a novel class of potent DHODH inhibitor effective against AML proliferations, promoting differentiation in these cells. Given the unmet need for managing AML, SBL-105 and its analogs warrant value for further testing and development in myeloid malignancies.

ACKNOWLEDGMENTS: *The authors extend appreciation to the Deanship of Scientific Research at King Khalid University, Abha, Saudi Arabia, for funding this work through grant number R.G.P.1/250/42. The authors express their gratitude to SMARTBIO LABS, Chennai-78, Tamil Nadu, India, and SiBIOLEAD, Chennai-44, Tamil Nadu, India, for the help rendered in this study. The authors declare no conflicts of interest.*

REFERENCES

1. Sykes DB. 2018. The emergence of dihydroorotate dehydrogenase (DHODH) as a therapeutic target in acute myeloid leukemia. Exp Opin Ther Targets 22(11):893–898.
2. Young JD, Yao SY, Baldwin JM, Cass CE, Baldwin SA. 2013. The human concentrative and equilibrative nucleoside transporter families, SLC28 and SLC29. Mol Aspects Med. 34(2–3):529–547.
3. Brown KK, Spinelli JB, Asara JM, Toker A. 2017. Adaptive reprogramming of de novo pyrimidine synthesis is a metabolic vulnerability in triple-negative breast cancer. Cancer Discov. 7(4):391–399.
4. Mathur D, Stratikopoulos E, Ozturk S, Steinbach N, Pegno S, Schoenfeld S, Yong R, Murty VV, Asara JM, Cantley LC, Parsons R. 2017. PTEN regulates glutamine flux to pyrimidine synthesis and sensitivity to dihydroorotate dehydrogenase inhibition. Cancer Discov. 7(4):380–390.
5. Koundinya M, Sudhalter J, Courjaud A, Lionne B, Touyer G, Bonnet L, Menguy I, Schreiber I, Perrault C, Vougier S, Benhamou B, Zhang B, He T, Gao Q, Gee P, Simard D, Castaldi MP, Tomlinson R, Reiling S, Barrague M, Newcombe R, Cao H, Wang Y, Sun F, Murtie J, Munson M, Yang E, Harper D, Bouaboula M, Pollard J, Grepin C, Garcia-Echeverria C, Cheng H, Adrian F, Winter C, Licht S, Cornella-Taracido I, Arrebola R, Morris A. 2018. Dependence on the pyrimidine biosynthetic enzyme DHODH is a synthetic lethal vulnerability in mutant KRAS-driven cancers. Cell Chem Biol. 25(6):705–717.e711.
6. Leban J, Vitt D. 2011. Human dihydroorotate dehydrogenase inhibitors, a novel approach for the treatment of autoimmune and inflammatory diseases. Arzneimittel-Forschung 61(1):66–72.
7. Dembitz V, Lalic H, Kodvanj I, Tomic B, Batinic J, Dubravcic K, Batinic D, Bedalov A, Visnjic D. 2020. 5-Aminoimidazole-4-carboxamide ribonucleoside induces differentiation in a subset of primary acute myeloid leukemia blasts. BMC Cancer 20(1):1090.
8. Prasanna Rajagopalan A-RM, AU-Aseeri Hateem, AU-Helal Ismail M, AU-Elbessoumy Ashraf A. 2018. IOX-101, a novel small molecule, reduces AML cell proliferation by Akt enzyme inhibition. Arch Biol Sci. 70(2):321–327.

9. Fathi AT, Karp JE. 2009. New agents in acute myeloid leukemia: Beyond cytarabine and anthracyclines. Curr Oncol Rep. 11(5):346–352.
10. Peters GJ, Schwartsmann G, Nadal JC, Laurensse EJ, van Groeningen CJ, van der Vijgh WJ, Pinedo HM. 1990. In vivo inhibition of the pyrimidine de novo enzyme dihydroorotic acid dehydrogenase by brequinar sodium (DUP-785; NSC 368390) in mice and patients. Cancer Res. 50(15):4644–4649.
11. Natale R, Wheeler R, Moore M, Dallaire B, Lynch W, Carlson R, Grillo-Lopez A, Gyves J. 1992. Multicenter phase II trial of brequinar sodium in patients with advanced melanoma. Ann Oncol. 3(8):659–660.
12. Sainas S, Giorgis M, Circosta P, Gaidano V, Bonanni D, Pippione AC, Bagnati R, Passoni A, Qiu Y, Cojocaru CF, Canepa B, Bona A, Rolando B, Mishina M, Ramondetti C, Buccinnà B, Piccinini M, Houshmand M, Cignetti A, Giraudo E, Al-Karadaghi S, Boschi D, Saglio G, Lolli ML. 2021. Targeting acute myelogenous leukemia using potent human dihydroorotate dehydrogenase inhibitors based on the 2-hydroxypyrazolo[1,5-a]pyridine scaffold: Sar of the biphenyl moiety. J Med Chem. 64(9):5404–5428.
13. Huang M, Wang Y, Collins M, Mitchell BS, Graves LM. 2002. A77 1726 induces differentiation of human myeloid leukemia K562 cells by depletion of intracellular ctp pools. Mol Pharmacol. 62(3):463–472.
14. Baumann P, Mandl-Weber S, Völkl A, Adam C, Bumeder I, Oduncu F, Schmidmaier R. 2009. Dihydroorotate dehydrogenase inhibitor a771726 (leflunomide) induces apoptosis and diminishes proliferation of multiple myeloma cells. Mol Cancer Ther. 8(2):366–375.
15. White RM, Cech J, Ratanasirintrawoot S, Lin CY, Rahl PB, Burke CJ, Langdon E, Tomlinson ML, Mosher J, Kaufman C, Chen F, Long HK, Kramer M, Datta S, Neuberg D, Granter S, Young RA, Morrison S, Wheeler GN, Zon LI. 2011. Dhodh modulates transcriptional elongation in the neural crest and melanoma. Nature 471(7339):518–522.
16. Rajagopalan P, Dera A, Abdalsamad MR, Chandramoorthy HC. 2019. Rational combinations of indirubin and arylidene derivatives exhibit synergism in human non-small cell lung carcinoma cells. J Food Biochem. 43(7):e12861.
17. Munier-Lehmann H, Vidalain PO, Tangy F, Janin YL. 2013. On dihydroorotate dehydrogenases and their inhibitors and uses. J Med Chem. 56(8):3148–3167.
18. Noe DA, Rowinsky EK, Shen HS, Clarke BV, Grochow LB, McGuire WB, Hantel A, Adams DB, Abeloff MD, Ettinger DS et al. 1990. Phase I and pharmacokinetic study of brequinar sodium (NSC 368390). Cancer Res. 50(15):4595–4599.
19. Zhang C, Chu M. 2018. Leflunomide: A promising drug with good antitumor potential. Biochem Biophys Res Commun. 496(2):726–730.
20. Takao K, Yamashita M, Yashiro A, Sugita Y. 2016. Synthesis and biological evaluation of 3-benzylidene-4-chromanone derivatives as free radical scavengers and α-glucosidase inhibitors. Chem Pharm Bull. (Tokyo) 64(8):1203–1207.
21. Livingstone R. 1963. Naturally occurring oxygen ring compounds. Nature 200(4906):509–509.
22. Kabbe H-J, Widdig A. 1982. Synthesis and reactions of 4-chromanones. Angewandte Chemie International Edition in English 21(4):247–256.
23. Christian S, Merz C, Evans L, Gradl S, Seidel H, Friberg A, Eheim A, Lejeune P, Brzezinka K, Zimmermann K, Ferrara S, Meyer H, Lesche R, Stoeckigt D, Bauser M, Haegebarth A, Sykes DB, Scadden DT, Losman J-A, Janzer A. 2019. The novel dihydroorotate dehydrogenase (DHODH) inhibitor bay 2402234 triggers differentiation and is effective in the treatment of myeloid malignancies. Leukemia 33(10):2403–2415.
24. Liu L, Dong Z, Lei Q, Yang J, Hu H, Li Q, Ji Y, Guo L, Zhang Y, Liu Y, Cui H. 2017. Inactivation/deficiency of DHODH induces cell cycle arrest and programed cell death in melanoma. Oncotarget 8(68):112354–112370.
25. Prasanna R, Harish CC. 2010. Anticancer effect of a novel 2-arylidene-4,7-dimethyl indan-1-one against human breast adenocarcinoma cell line by G_2/M cell cycle arrest. Oncol Res. 18(10):461–468.
26. de Thé H. 2018. Differentiation therapy revisited. Nat Rev Cancer. 18(2):117–127.
27. Wu D, Wang W, Chen W, Lian F, Lang L, Huang Y, Xu Y, Zhang N, Chen Y, Liu M, Nussinov R, Cheng F, Lu W, Huang J. 2018. Pharmacological inhibition of dihydroorotate dehydrogenase induces apoptosis and differentiation in acute myeloid leukemia cells. Haematologica 103(9):1472–1483.
28. Zeng Z, Konopleva M. 2018. Targeting dihydroorotate dehydrogenase in acute myeloid leukemia. Haematologica 103(9):1415–1417.
29. Heo SK, Noh EK, Yoon DJ, Jo JC, Choi Y, Koh S, Baek JH, Park JH, Min YJ, Kim H. 2015. Radotinib induces apoptosis of CD11b+ cells differentiated from acute myeloid leukemia cells. PloS One 10(6):e0129853.
30. Xu S, Li X, Zhang J, Chen J. 2015. Prognostic value of cd11b expression level for acute myeloid leukemia patients: A meta-analysis. PloS One 10(8):e0135981.
31. Gaidano V, Houshmand M, Vitale N, Carrà G, Morotti A, Tenace V, Rapelli S, Sainas S, Pippione AC, Giorgis M, Boschi D, Lolli ML, Cilloni D, Cignetti A, Saglio G, Circosta P. 2021. The synergism between dhodh inhibitors and dipyridamole leads to metabolic lethality in acute myeloid leukemia. Cancers (Basel) 13(5):1003.
32. Peters GJ, Kraal I, Pinedo HM. 1992. In vitro and in vivo studies on the combination of brequinar sodium (DUP-785; NSC 368390) with 5-fluorouracil; effects of uridine. Br J Cancer 65(2):229–233.